

Effects of multiple scattering on attenuation-based retrievals of stratiform rainfall from CloudSat

*Original*

Effects of multiple scattering on attenuation-based retrievals of stratiform rainfall from CloudSat / Matrosov, S.Y., Battaglia, A., Rodriguez, P.. - In: JOURNAL OF ATMOSPHERIC AND OCEANIC TECHNOLOGY. - ISSN 1520-0426. - 25:12(2008), pp. 2199-2208. [10.1175/2008JTECHA1095.1]

*Availability:*

This version is available at: 11583/2807860 since: 2020-03-31T23:17:16Z

*Publisher:*

AMER METEOROLOGICAL SOC

*Published*

DOI:10.1175/2008JTECHA1095.1

*Terms of use:*

This article is made available under terms and conditions as specified in the corresponding bibliographic description in the repository

*Publisher copyright*

(Article begins on next page)

# Effects of Multiple Scattering on Attenuation-Based Retrievals of Stratiform Rainfall from CloudSat

SERGEY Y. MATROSOV

*Cooperative Institute for Research in Environmental Sciences, University of Colorado, and NOAA/Earth System Research Laboratory, Boulder, Colorado*

ALESSANDRO BATTAGLIA

*Meteorological Institute, University of Bonn, Bonn, Germany*

PETER RODRIGUEZ

*Environment Canada, King City, Ontario, Canada*

(Manuscript received 26 November 2007, in final form 25 April 2008)

## ABSTRACT

An attenuation-based method to retrieve vertical profiles of rainfall rates from height derivatives/gradients of CloudSat nadir-pointing W-band reflectivity measurements is discussed. This method takes advantage of the high attenuation of W-band frequency signals in rain and the low variability of nonattenuated reflectivity due to strong non-Rayleigh scattering from rain drops. The retrieval uncertainties could reach 40%–50%. The suggested method is generally applicable to rainfall rates ( $R$ ) in an approximate range from about 2–3 to about 20–25  $\text{mm h}^{-1}$ . Multiple scattering noticeably affects the gradients of CloudSat measurements for  $R$  values greater than about 5  $\text{mm h}^{-1}$ . To avoid a retrieval bias caused by multiple-scattering effects, a special correction for retrievals is introduced. For rainfall rates greater than about 25  $\text{mm h}^{-1}$ , the influence of multiple scattering gets overwhelming, and the retrievals become problematic, especially for rainfalls with higher freezing-level altitudes. The attenuation-based retrieval method was applied to experimental data from CloudSat covering the range of rainfall rates. CloudSat retrievals were compared to the rainfall estimates available from a National Weather Service ground-based scanning precipitation radar operating at S band. Comparisons between spaceborne and conventional radar rainfall retrievals were generally in good agreement and indicated the mutual consistency of both quantitative precipitation estimate types. The suggested CloudSat rainfall retrieval method is immune to the absolute calibration of the radar and to attenuation caused by the melting layer and snow regions. Since it does not require surface returns, it is applicable to measurements above both land and water surfaces.

## 1. Introduction

The CloudSat satellite, launched in 2006, carries the world's first nadir-pointing W-band (94 GHz) cloud profiling radar (CPR) in space. The first year of CloudSat operations provided unique global information on atmospheric hydrometeors (e.g., Mace et al. 2007). W-band frequencies are the highest used in radar remote sensing, and signals at these frequencies experience the strongest atmospheric attenuation, especially in rainfall. Although the main objective of the CPR is to pro-

vide quantitative information on clouds, it has been suggested previously that its data also can be used to retrieve snowfall and light rainfall parameters where the signal attenuation is not very severe (e.g., L'Ecuyer and Stephens 2002; Stephens et al. 2002; Matrosov 2007a; Matrosov et al. 2008).

Radar rainfall retrieval methods at attenuating radar frequencies have a rather long history (e.g., Hirschfeld and Bordan 1954). Typically, these methods account for attenuation along the radar beam using special approaches and reconstruct a profile of nonattenuated equivalent radar reflectivity factor  $Z_e$  (hereafter just "reflectivity"). Sometimes, constraints are used when total attenuation values along the radar beam are available either from surface returns or from polarimetric

---

*Corresponding author address:* Sergey Matrosov, R/PSD2, 325 Broadway, Boulder, CO 80305.  
E-mail: sergey.matrosov@noaa.gov

measurements (e.g., Meneghini et al. 2000; Testud et al. 2000). Most of the existing methods rely on relations between rain rate  $R$  (and also the attenuation coefficient  $\alpha$ ) and nonattenuated reflectivity  $Z_e$ . The use of attenuating frequencies for rainfall measurements is common at X band (wavelength  $\lambda \sim 3$  cm) for scanning radars (e.g., Matrosov et al. 2005) and  $K_u$  band ( $\lambda \sim 2$  cm) for vertically (nadir) pointing radars such as the Tropical Rainfall Measuring Mission (TRMM) radar (e.g., Iguchi et al. 2000).

At W-band frequencies, attenuation becomes a dominant factor responsible for vertical changes in measured reflectivities  $Z_{em}$ , observed along the radar beam for  $R$  values greater than several millimeters per hour. On the other hand, for  $R > 3\text{--}4$  mm h<sup>-1</sup>, the variability of nonattenuated reflectivities  $Z_e$  with respect to  $R$  (and also  $\alpha$ ) becomes relatively insignificant due to strong non-Rayleigh scattering effects (Matrosov 2007b). These factors make the use of existing methods of rainfall estimation at attenuating radar frequencies not very practical at W band except for very light rainfall.

A novel attenuation-based approach for rainfall estimations from CloudSat measurements was recently suggested (Matrosov 2007b). Under this approach, the changes in the vertical profile of observed  $Z_{em}$  due to attenuation are treated as a useful signal, while other factors such as the vertical variability of nonattenuated reflectivity at the resolution intervals ( $\sim 1$  km or so) are considered as factors contributing to the retrieval uncertainty. Although a version of this approach was first applied to vertically pointing  $K_a$ -band radars (Matrosov et al. 2006), its application to W band has the advantage of much smaller changes in  $Z_e$  due to  $R$  and significantly stronger attenuation due to rain. The variability in drop size distributions (DSDs), however, has a stronger effect on the retrieval accuracy at W-band frequencies than at  $K_a$ -band frequencies.

A relatively large CPR footprint ( $\sim 1.5$  km) results in multiple-scattering contributions that increase with  $R$  and affect CloudSat measurements (Battaglia et al. 2007). The initial version of the attenuation-based method, as practically all other radar rainfall retrieval methods, is based on the single-scattering (SS) assumption. It has been shown, however, that this method as applied to the CloudSat data provides reasonable retrievals for rain rates in a range  $R \sim 2\text{--}5$  mm h<sup>-1</sup> (Matrosov 2007b). In this study, the attenuation-based algorithm is extended to higher rain rates, and the multiple-scattering corrections are introduced. The CloudSat retrieval results are then compared to the estimates obtained with weather surveillance ground-based radars, which are the traditional tool for remote

rainfall observations and quantitative precipitation estimations (QPEs).

## 2. A description of the attenuation-based gradient method for CloudSat

The attenuation-based method retrieves vertical profiles of rainfall rates under an assumption that changes of measured reflectivity in rain (i.e.,  $Z_{em}$ ) at a vertical interval  $\Delta h$  are dominated by attenuation in rain, and the variability of nonattenuated reflectivity  $\delta Z_e$  at this interval is smaller compared to changes due to attenuation. This variability contributes to the uncertainty of the retrieval. Due to non-Rayleigh scattering at W-band frequencies,  $\delta Z_e$  typically does not exceed a few decibels for rainfall rates greater than about 3–4 mm h<sup>-1</sup> (Matrosov 2007b).

Assuming single scattering and the dominance of attenuation in shaping vertical trends of observed reflectivity, the one-way attenuation coefficient in rain  $\alpha(h)$  is estimated from the vertical gradient of the measured reflectivity,  $\partial Z_{em}(h)/\partial h$ , in a rain layer as

$$\alpha(h) = (1/2)[\partial Z_{em}(h)/\partial h] - G(h), \quad (1)$$

where the coefficient  $1/2$  accounts for the two-way propagation, and  $G(h)$  is the gaseous ( $O_2$  and  $H_2O$ ) absorption coefficient correction, which is determined by the profiles of temperature, pressure, and relative humidity. It is assumed that hydrometeor attenuation is dominated by rain. Temperature and pressure profiles for calculating  $G(h)$  are available as auxiliary CloudSat information, and the relative humidity in the rain layer is assumed to be 95%. The melting layer feature often observed by CloudSat in precipitating systems (Sassen et al. 2007) is used to fine tune the temperature profile.

The gradient (i.e., the height derivative)  $\partial Z_{em}(h)/\partial h$  is estimated as a linear slope of the  $Z_{em}(h)$  vertical trend at  $n$  consecutive CloudSat sampling gates ( $\sim 0.24$  km) using the least squares method (LSM). It provides the effective vertical resolution of retrievals that corresponds to the height interval  $\Delta h = n \times 0.24$  km and is centered in the middle of this interval. The estimates of  $\alpha(h)$  using (1) are performed using “sliding range window,” so they are available with 0.24-km spacing. The CloudSat reflectivity data points that are below the radar receiver noise floor or are contaminated by the echoes from the ground or the melting layer are rejected. The estimates of  $\alpha(h)$  are deemed unreliable if more than half of  $n$  data points used to calculate the slope are rejected. It was shown (Matrosov 2007b) that  $n = 5$  generally provides satisfactory retrievals.

When the attenuation coefficient  $\alpha(h)$  is estimated

from (1), a corresponding rainfall rate is obtained using an  $\alpha$ - $R$  relation. While this relation is slightly nonlinear, the data scatter due to the DSD variability to a large extent masks this nonlinearity, and the following average linear relation satisfactorily describes a correspondence between  $\alpha$  and  $R$  at W band, at least for  $R$  values that are smaller than about  $20 \text{ mm h}^{-1}$ :

$$R (\text{mm h}^{-1}) \approx 1.2 k(h)\alpha (\text{dB km}^{-1}), \quad (2)$$

where the dimensionless coefficient  $k(h)$  accounts for the changes in drop terminal velocity due to changes with height in air density,  $\rho_a$  [ $k(h) = 1.1\rho_a(h)^{-0.45}$ ,  $\rho_a(h)$  in  $\text{kg m}^{-3}$ ].

Relation (2) was obtained by analyzing a large number of rain DSDs that were observed in both convective and stratiform rainfalls in different geographical areas and seasons (Matrosov 2007b). Note that changes in the  $\alpha$ - $R$  relations with temperature at millimeter wavelengths are significantly less than for centimeter wavelengths (Matrosov et al. 2006), and these changes can be largely neglected at W band when compared to the data scatter due to DSD variability.

The data scatter around (2) due to the DSD variability is about 35% (Matrosov 2007b). While this data scatter is substantially greater than that for  $K_a$  band, the strength of attenuation effects and a very low variability of nonattenuated reflectivity at W band compensate for this drawback and make the CloudSat attenuation-based retrievals of  $R$  a viable option for spaceborne quantitative rainfall estimations. The attenuation-based gradient method can be applicable for both convective and stratiform rains; however, retrieval errors in convective rains might be larger due to stronger spatial variability of such rains and a generally higher influence of multiple scattering. Stratiform rains, which typically result from snowflake melting, provide a more convenient target since they often offer a clear separation of rain and solid hydrometeor regions as viewed by CloudSat (e.g., Sassen et al. 2007). Since rainfall rates could vary in the vertical even for stratiform rains, the ability of the gradient method to resolve the vertical structure of rainfall adds to its usefulness. Two important advantages of the gradient method are that (a) it does not require absolute calibration of the radar data and (b) it is immune to the attenuation caused by the ice phase of precipitating systems and by melting hydrometers that are observed above the rain layer.

Under the single-scattering assumption, the two main contributions to the retrieval errors of the attenuation-based method are the uncertainty in relation (2) due to the DSD variability and the variability of nonattenuated reflectivity at the gradient estimation interval  $\Delta h$ .

Combination of these two factors results in possible retrieval errors of about 40%–50% for rain rates greater than about  $2 \text{ mm h}^{-1}$  (Matrosov 2007b). These errors decrease for heavier rainfalls as attenuation increases. They are comparable to the uncertainties of traditional reflectivity-based methods that are used with scanning precipitation radars, which operate at centimeter-wavelength frequencies (3–10 GHz). The retrieval errors for  $R < 2 \text{ mm h}^{-1}$  might increase beyond 50% because attenuation in lighter rains decreases, and the attenuation contribution (in a relative sense) due to cloud liquid increases. In addition, the variability of nonattenuated reflectivity increases for lighter rainfalls as the non-Rayleigh-scattering effects become less significant for such rains. The radar approaches that correct observed reflectivity for attenuation and then relate recovered nonattenuated reflectivity values to rainfall rates could be more appropriate than the attenuation-based gradient method for these lighter rains.

Unlike measurements from airborne W-band radars (e.g., Li et al. 2004), CloudSat observations, due to their relatively large spatial resolution, also have multiple-scattering contributions in measured echoes. These contributions become progressively stronger as the intensity of rainfall increases, and they hamper the application of the retrieval methods that assume single scattering (Battaglia and Simmer 2008). Multiple-scattering effects increase the power of the returned signals compared to what would have been observed under single-scattering conditions. These effects result in smaller vertical gradients (slopes) of measured reflectivity. It would bias low attenuation-based estimates of rainfall rates if no correction is applied. A procedure for correcting these effects is needed for successful applications of the attenuation-based gradient method to the CloudSat measurements.

### 3. The influence of multiple-scattering effects on slopes of CloudSat-measured reflectivity

CloudSat measurements in rain revealed an influence of multiple scattering on observed reflectivities. While it is impossible to assess multiple-scattering effects directly from measurements, modeling is one viable option to estimate the magnitude of these effects and to develop corrections that will account for multiple scattering in CloudSat retrieval algorithms. The Monte Carlo simulator for stratiform rain described by Battaglia and Simmer (2008) accounts for the CloudSat antenna and sampling characteristics, and it was used in this study to model CloudSat measurements in rain of

different intensities, assuming various heights of the freezing level (i.e., the height of the  $0^{\circ}\text{C}$  isotherm). Figure 1 shows comparisons of modeled attenuated reflectivity under conditions of single and multiple scattering. The geometry of CloudSat measurements (i.e., the orbit height and spatial resolution) was taken into account. The density of snow particles above the freezing-level (FL) height was assumed to be  $0.1\text{ g cm}^{-3}$ .

It can be seen from Fig. 1 that melting snowflakes immediately below the  $0^{\circ}\text{C}$  isotherm height are manifested by the brightband-like feature (Sassen et al. 2007), which is followed by the gradual decrease of reflectivities in the rain layer. This decrease is governed by attenuation under the single-scattering assumption and by the combination of attenuation and multiple-scattering effects when all degrees of scattering are considered. Multiple-scattering (MS) effects also cause the surface backscatter peak to diminish compared to the single-scattering (SS) case. For higher rainfall rates (e.g., Figs. 1c,d), this peak practically vanishes.

The MS contribution increases with rainfall rate (Fig. 1). It is only a couple of decibels for  $R = 2\text{ mm h}^{-1}$ , but it amounts to about 6–7 dB for  $R = 5\text{ mm h}^{-1}$  and to more than 12 dB for  $R = 15\text{ mm h}^{-1}$ . One remarkable feature is that while this contribution could be large in the absolute sense, the slope of the  $Z_{\text{em}}$  trend in the rain layer (i.e., the vertical gradient) changes significantly less (almost negligibly for  $R \leq 5\text{ mm h}^{-1}$ ). This feature can be explained by the fact that the net MS effect changes with height in the rain layer rather modestly, which is beneficial for the gradient method since it relies on the  $Z_{\text{em}}$  slopes and does not use the absolute reflectivity measurements.

Another remarkable feature is that the  $Z_{\text{em}}$  slopes in the rain layer are fairly insensitive to the assumption of the density of snowflakes observed above the FL. Figure 2 shows modeling results for two snowflake densities ( $0.1$  and  $0.18\text{ g cm}^{-3}$ ) and the resultant rainfall rate of  $9\text{ mm h}^{-1}$  with the FL height of  $4\text{ km}$ . It can be seen that the snowflake density assumption is important for the absolute values of  $Z_{\text{em}}$ , but the  $Z_{\text{em}}$  slopes change very little with variations of  $\rho_s$ . This conclusion remains valid for a broad range of resultant rainfall rates ( $R < 25\text{ mm h}^{-1}$ ) and freezing level heights ( $\text{FL} \leq 5\text{ km}$ ). It should be mentioned, however, that  $Z_{\text{em}}$  slopes become sensitive to the  $\rho_s$  assumption for very high values of  $\rho_s$  ( $\sim 0.5\text{ g cm}^{-3}$  or so), which are more representative of graupel than of aggregated snowflakes with a limited degree of riming.

The presented modeling data indicate that the influence of MS effects on the attenuation-based gradient method retrievals might be rather modest for light to

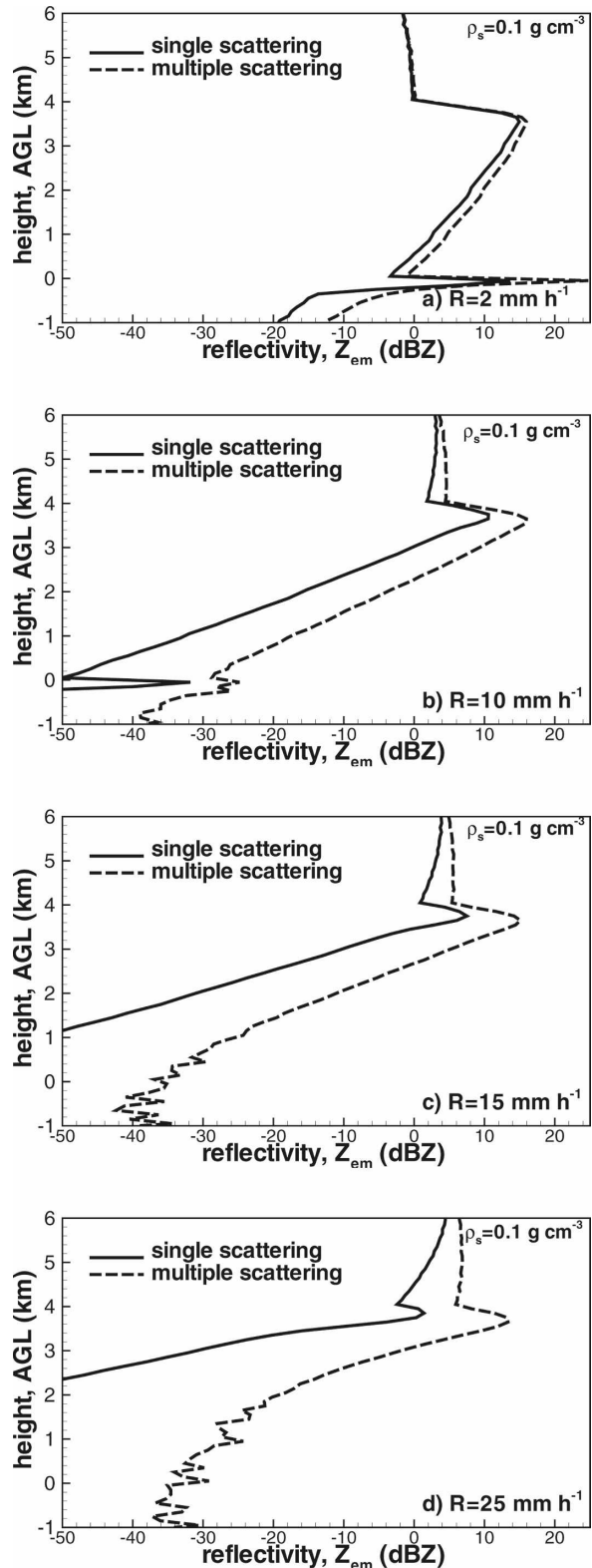


FIG. 1. Comparisons of single- and multiple-scattering simulated CloudSat profiles for different rainfall rates: (a) 2, (b) 10, (c) 15, and (d) 25  $\text{mm h}^{-1}$ ; FL = 4 km.

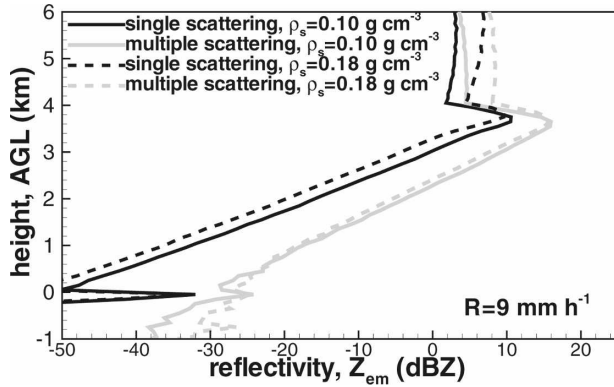


FIG. 2. Vertical profiles of simulated CloudSat reflectivity under assumptions of single and multiple scattering for snowflake densities of 0.10 and 0.18 g cm<sup>-3</sup>; FL = 4 km.

moderate rainfall rates. It can be seen, for example, that smaller values of  $R$  slopes change relatively little (Fig. 1), but for  $R = 15 \text{ mm h}^{-1}$  the slope change is already noticeable. The difference in SS and MS slopes is even higher for  $R = 25 \text{ mm h}^{-1}$ . This change gets more pronounced toward the bottom of the rain layer, where the slope becomes progressively smaller compared to the higher levels in the rain layer. Since the decrease of the  $Z_{em}$  slope due to MS effects becomes stronger as  $R$  gets larger, an introduction of the correction factor for the observed  $Z_{em}$  slope is reasonable before applying the attenuation-based gradient retrieval method.

As rainfall rate increases and MS contributions become stronger, the changes in vertical profiles of  $Z_{em}$  become progressively less pronounced. This is seen from Fig. 3, in which results of the Monte Carlo simulations are shown for different values of rainfall rates and FL heights. For low FL values [e.g., FL = 2 km (Fig. 3d)] the slope of the  $Z_{em}$  trend becomes monotonically steeper when  $R$  increases over the rainfall-rate range between 0 and 30 mm h<sup>-1</sup>. At higher FL values [e.g., FL = 5 km (Fig. 3a) and FL = 4 km (Fig. 3b)], the slopes and the absolute values practically do not change for  $R > 25 \text{ mm h}^{-1}$ , which indicates that CloudSat retrievals for such rains are problematic using any approach. The MS effects are the strongest for heavier rainfalls in lower parts of the rain layer. An increased statistical noise of modeling data is observed in these areas. Note that MS is also responsible for echoes that are observed at the ranges exceeding the distance to the ground, which is assumed to be at 0-km height.

As mentioned before, MS reduces the surface backscatter peak and eventually removes it as the rainfall rate becomes larger and/or the rain layer becomes thicker. While the absence of the surface peak is an almost sure indication of the presence of MS effects, its

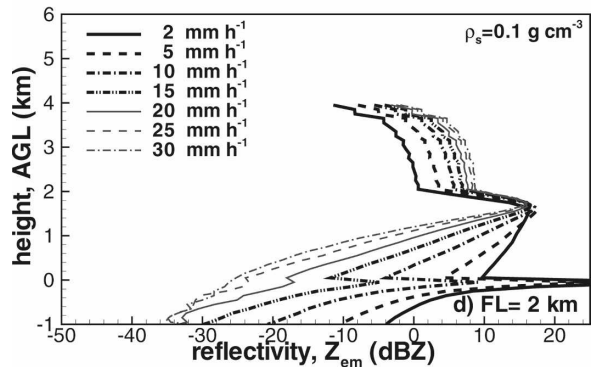
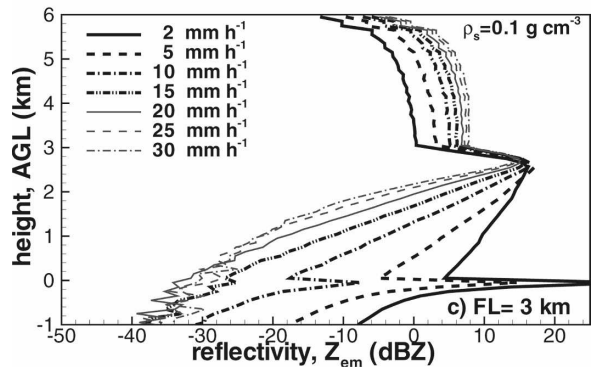
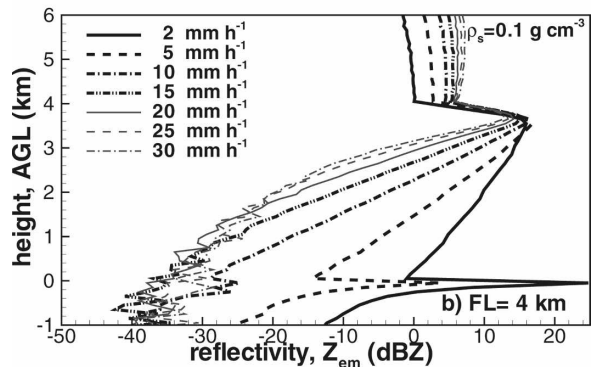
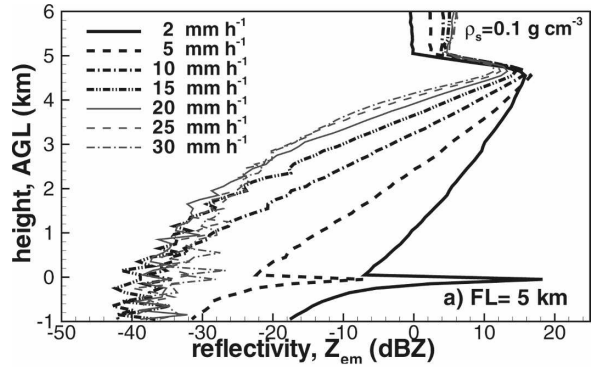


FIG. 3. Simulations of CloudSat profiles with accounting for MS effects for different FL heights: (a) 5, (b) 4, (c) 3, and (d) 2 km.

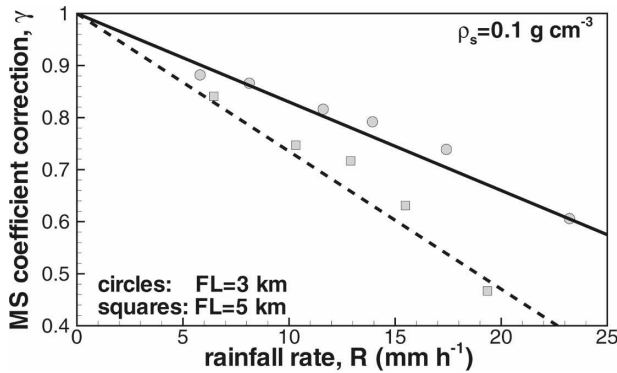


FIG. 4. Results of calculations of the MS correction parameter  $\gamma$  as function of rainfall rate at different FL heights.

existence does not necessarily mean the absence of these effects for absolute reflectivities, as seen, for example, in Fig. 1b. The mean rainfall rate in the rain layer and, to a somewhat lesser extent, the thickness of this layer are the two main parameters that determine the relative strength of MS effects that influence the slope of the vertical trend in observed CloudSat reflectivities.

#### 4. A multiple-scattering correction for the $Z_{em}$ slopes and its application

##### a. Derivation of the MS correction

A multiple-scattering correction parameter  $\gamma$  for the attenuation-based gradient rainfall retrieval method is defined as

$$[\partial Z_{em}(h)/\partial h]_{ms} = \gamma [\partial Z_{em}(h)/\partial h]_{ss}, \quad (3)$$

where subscripts ms and ss stand for multiple and single scattering, respectively. The reciprocal of this parameter,  $\gamma^{-1}$ , scales the slope of the observed (i.e., attenuated) CloudSat reflectivity trend modified by the effects of multiple scattering to the slope that would be observed if only single scattering were present. The parameter  $\gamma$  diminishes as rainfall rate increases. Multiple-scattering effects are absent if  $R = 0$ , so  $\gamma = 1$  then. For  $R < 5 \text{ mm h}^{-1}$ ,  $\gamma$  is usually greater than 0.9, indicating that the MS corrections are generally less than about 10%. The parameter  $\gamma$  also depends on the FL height, because MS gets more pronounced as the rain-layer thickness increases. It also depends on the location within this layer, as MS effects are stronger in the areas that are closer to the ground.

Figure 4 shows an example of  $\gamma$  calculations as a function of rainfall rate for FL heights of 3 and 5 km. The  $\gamma$  values correspond to the middle of the rain layer. While some amount of statistical noise is present in the

Monte Carlo calculations, there is an approximately linear trend of  $\gamma$  as a function of  $R$ :

$$\gamma \approx 1 - aR, \quad (4)$$

where the coefficient  $a$  is a function of the FL height.

The best linear fit relations for  $\gamma$  were calculated for different values of the FL heights. The corresponding values of  $a$  are 0.012, 0.017, 0.022, and 0.027  $\text{mm h}^{-1}$  for the FL heights of 2, 3, 4, and 5 km, respectively. While these values were obtained for the snowflake density  $\rho_s = 0.1 \text{ g cm}^{-3}$ , the corresponding MS corrections are generally representative for rainfalls resulting from melting snowflakes that have only a light or moderate degree of riming. This occurs because the MS influence on the slope of  $Z_{em}$  trends varies with snowflake density rather little for densities that are typical for such riming (i.e.,  $\rho_s$  less than about 0.2–0.3  $\text{g cm}^{-3}$ ). The variability of  $\gamma$  for such snow densities is negligible for  $R < 10 \text{ mm h}^{-1}$ , and it is generally within 15%–20% for  $15 \text{ mm h}^{-1} < R < 20 \text{ mm h}^{-1}$ . For heavily rimed snow (e.g., graupel), MS effects are stronger, and they will require greater corrections, which, probably, should depend on the snowflake density.

Data in Fig. 4 also correspond to the CloudSat resolution gate, which is located in the middle of the rain layer. There is no significant variability in data depending on the gate location inside the rain layer for lower rain rates ( $R < 10 \text{ mm h}^{-1}$ ). However, for thick rain layers (FL  $\geq 3 \text{ km}$ ) and heavier rainfalls, the coefficient  $a$  in (4) decreases by about 15% from values that correspond to the data in Fig. 4 for the gates that are in the vicinity of the melting layer. For such rainfalls, the MS effects on  $Z_{em}$  slopes become progressively stronger as the radar signals penetrate deeper into a scattering medium. Consequently, values of  $a$  for lower parts of the rain layer should increase compared to those that are suited for the upper and middle parts of the rain layer. For shallower rains, the variability in the coefficient  $a$ , depending on the location of the resolution volume in the rain layer, is rather small and, most likely, can be neglected for many practical cases. The modeling results indicate that the MS correction parameter  $\gamma$  is generally larger than 0.5 (i.e., the slopes of the  $Z_{em}$  vertical trends are usually not changed due to MS by more than a factor of 2) for  $R < 20 \text{ mm h}^{-1}$  and FL  $\leq 5 \text{ km}$ .

##### b. Application of the method with MS corrections

Since the multiple-scattering correction parameter  $\gamma$  depends on rainfall rate, the CloudSat rainfall retrievals are performed in an iterative way. First, a profile of  $R$  is retrieved under the single-scattering assumption from

(1) and (2), and a mean value of rainfall rate  $R_a$  for this profile is calculated. As discussed in section 4, an appropriate value of  $\gamma$  is then chosen based on the value of  $R_a$  and the information about the FL height and the location of the resolution gate within a profile. The corrected SS slopes are then calculated using (3) with the appropriate  $\gamma$ , and the new profile is retrieved from (1) and (2). The next value of  $R_a$  is then calculated for this iteration. The iterations are stopped when values of  $R_a$  does not change by more than 10%. Given that the overall retrieval uncertainties are noticeably higher, the threshold of 10% appears to be justified. Typically, one or two iterations are enough to satisfy this condition.

As MS effects reduce the slopes of  $Z_{em}$  vertical trends, the net MS correction increases retrieved rainfall rates compared to the results obtained under the SS assumption. Both MS and SS slopes monotonically increase with  $R$  for  $R$  values in an interval between 0 and about  $25 \text{ mm h}^{-1}$  (for  $R \leq 30 \text{ mm h}^{-1}$  in case of shallower rains), and there is generally no ambiguity in the retrieved values within this interval. Since the MS reflectivity slopes change very little for higher rainfall rates in a precipitating system with  $FL \approx 4 \text{ km}$  were of the order of  $4\text{--}5 \text{ mm h}^{-1}$ . The CloudSat results were consistent with observations of the ground-based scanning precipitation radars that operate at S band ( $\sim 3 \text{ GHz}$ ). It can be seen from Fig. 4 that MS corrections for such rainfall rates are expected to be within 10%. These corrections are small compared to the overall retrieval uncertainty, and the introduction of the MS correction would not significantly change the results shown in (Matrosov 2007b).

It should be mentioned that some additional retrieval uncertainties might be introduced because the mean layer rainfall rate  $R_a$  is used for calculating  $\gamma$ . If the variability in  $R$  within a rain layer is  $\pm 25\%$ , for example, then for the strongest MS contaminations for which retrievals are performed (e.g.,  $FL = 5 \text{ km}$ ,  $R \sim 15\text{--}25 \text{ mm h}^{-1}$ ), uncertainty in  $\gamma$  can be as high as about 20% from the mean value of 0.5 (at  $R \approx 20 \text{ mm h}^{-1}$ ), as seen from Fig. 4. A resultant additional retrieval error for  $R$  could be of approximately the same amount ( $\sim 20\%$ ), which is still noticeably smaller than possible retrieval uncertainties due to variability of DSDs and nonattenuated reflectivities ( $\sim 40\%$ ). Nevertheless, it could be stated that the suggested procedure of introducing MS corrections is better suited to stratiform rains, where the variability of rainfall rates below the melting layer is usually not very significant. For such rains, a typical variability of Rayleigh reflectivities is only 1–2 dB, and a corresponding variability in rainfall rates is usually smaller than that of reflectivity (e.g., Bellon et al. 2006; Matrosov et al. 2007).

### 5. Illustrations of the CloudSat rainfall retrievals with MS correction

The first CloudSat rainfall retrievals using the attenuation-based gradient method were presented by Ma-

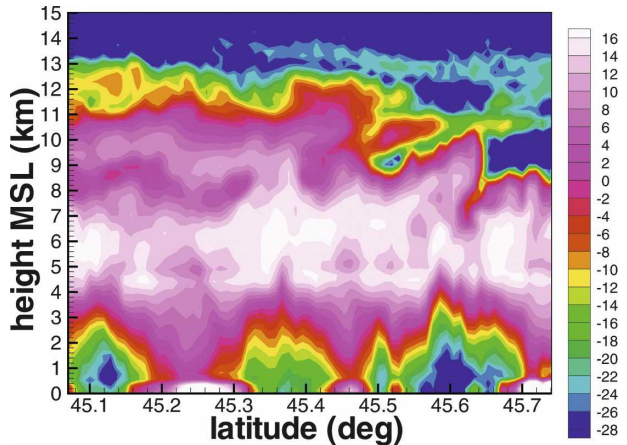


FIG. 5. A cross section of the CloudSat measurements observed on 2 Aug 2006 when the satellite passed near the Wisconsin–Michigan border.

trosov (2007b). The MS effects were not considered during these retrievals and typical observed rainfall rates in a precipitating system with  $FL \approx 4 \text{ km}$  were of the order of  $4\text{--}5 \text{ mm h}^{-1}$ . The CloudSat results were consistent with observations of the ground-based scanning precipitation radars that operate at S band ( $\sim 3 \text{ GHz}$ ). It can be seen from Fig. 4 that MS corrections for such rainfall rates are expected to be within 10%. These corrections are small compared to the overall retrieval uncertainty, and the introduction of the MS correction would not significantly change the results shown in (Matrosov 2007b).

It is instructive to analyze cases with higher rainfall rates when the MS correction is relatively more important. Simultaneous rainfall observations from the ground-based precipitation radars are also helpful, as they can be compared with CloudSat results. Comparisons of spaceborne and surface-based rainfall measurements cannot be regarded as a strict validation effort because of relatively high retrieval errors for both types of measurements. Such comparisons, however, provide a useful consistency check for CloudSat retrievals because surface weather radars and CloudSat have comparable sample volumes, and these radars have a long history of QPE studies.

A cross section of measured radar reflectivities from CloudSat,  $Z_{em}$ , as it passed on 2 August 2006 over a precipitating system in the vicinity of Green Bay near the Wisconsin–Michigan border is shown in Fig. 5. This overpass occurred over the waters of Lake Michigan and over the land in Michigan's Upper Peninsula. The brightband features for this event can be seen near 4.5 km MSL. While the signal attenuation due to rain below 4 km MSL is evident for the entire latitude interval

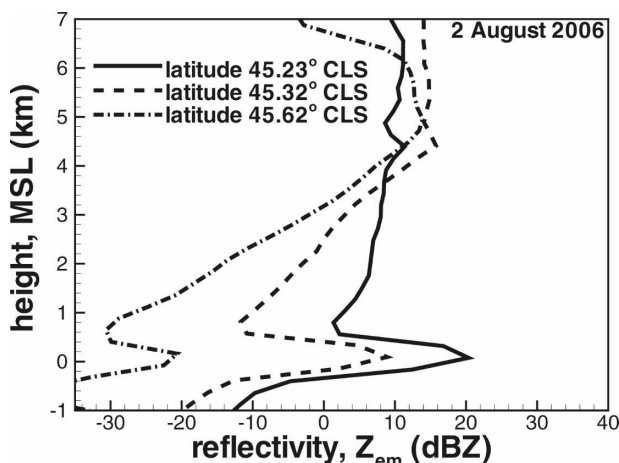


FIG. 6. Vertical profiles of CloudSat reflectivities observed on 2 Aug 2006.

in Fig. 5, there are areas of differing attenuation rates that are related to the horizontal variability in rainfall.

For this rainfall event, Fig. 6 shows three representative CloudSat reflectivity profiles that correspond to various rainfall intensities. The brightband features in the upper part of the melting layer are quite visible, though they are not very pronounced. The vertical positions of reflectivity enhancements within the melting layer vary only slightly. While presented profiles are characterized by similar reflectivity values in the first 1-km layer above the melting layer, the slopes of the reflectivity gradient below this layer differ very significantly, with heavier rainfall resulting in steeper vertical gradients of observed values of  $Z_{em}$ .

The W-band attenuation-based method was used to retrieve rainfall rates from CloudSat measurements presented in Fig. 5. For the most part, this event could probably be considered as stratiform, except for some possible embedded convective cells (e.g., at a latitude around 45.14°). Figure 7a shows how the corresponding CloudSat retrievals compare to the nearby Weather Surveillance Radar-1988 Doppler (WSR-88D) estimates. This National Weather Service radar operates at S-band frequency, and its signals are essentially nonattenuated. It is located near Green Bay, Wisconsin, and has the four-letter identifier KGRB. The standard S-band  $Z_e$ - $R$  relation ( $Z_e = 300R^{1.4}$ ), which is often used with WSR-88D Next Generation Weather Radar (NEXRAD) network data, was applied to the KGRB data.

The WSR-88D radar estimates in Fig. 7a were compiled from measurements at beam elevation tilts between 0.9° and 1.7°. The range resolutions of KGRB estimates are 1 km, and the WSR-88D radar beamwidth of about 1° could result in vertical resolutions of

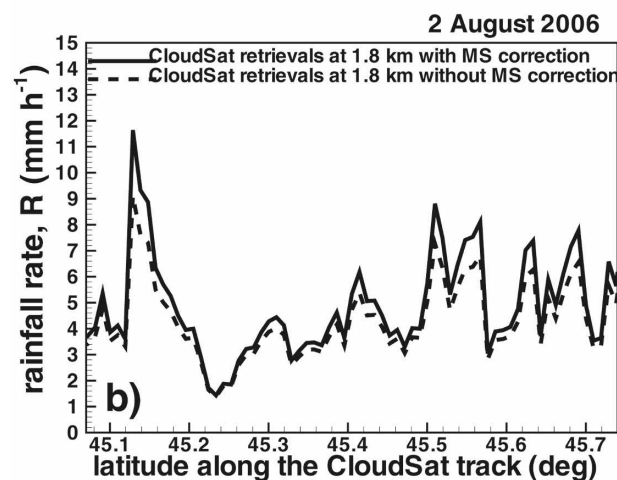
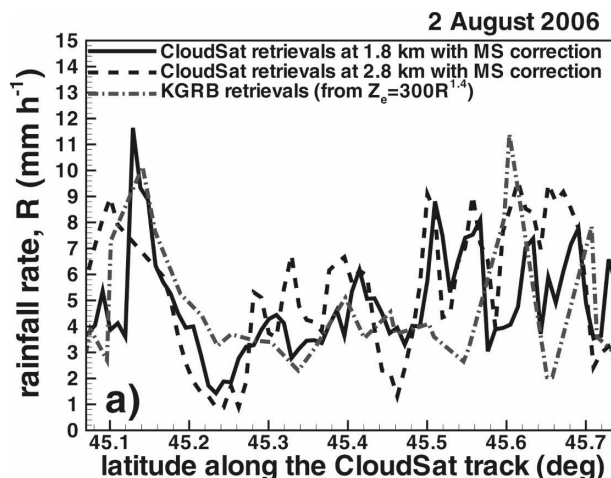


FIG. 7. Comparisons of (a) CloudSat and KGRB NEXRAD rainfall-rate retrievals and (b) CloudSat retrievals with and without MS corrections.

1–2 km at the observed distances between CloudSat samples and the KGRB radar. The time mismatch between CloudSat and KGRB values is about 1 min. To provide a sense of vertical variability of the observed rainfall, satellite retrievals are shown at the heights centered at 1.8 and 2.8 km MSL. It can be seen that the vertical changes of rainfall are generally within the CloudSat retrieval uncertainties. Comparisons with the ground-based radar results are also quite favorable given these uncertainties and also uncertainties of NEXRAD estimates. The NEXRAD estimate uncertainties associated with the variability of S-band  $Z_e$ - $R$  relations could be as high as a factor of 2.

Figure 7b illustrates the importance of the MS scattering correction for the event of 2 August 2006. As mentioned before, correction values are noticeably smaller than expected retrieval uncertainties for lighter rainfall rates (less than about 5 mm h<sup>-1</sup>), and they

probably can be neglected. For higher rainfall rates, MS corrections become appreciable. Not accounting for MS effects for such rainfall rates might lead to noticeable retrieval biases, resulting in underestimation of rainfall. It should be noted also that while some rainfall peaks observed during this event (e.g., in the vicinity of N 45.14°) might be associated with convection activities, the MS correction for CloudSat attenuation-based retrievals provides sensible results here. However, the question of applicability and the appropriateness of MS corrections, which were proposed here for stratiform rainfalls, for convective rainfalls remains an outstanding issue and needs to be addressed in the future.

## 6. Summary and conclusions

The attenuation-based method to retrieve vertical profiles of rainfall rate from nadir-pointing radar data from the CloudSat satellite has been described. This method takes advantage of the strong attenuation of W-band radar signals in rain and the low variability of nonattenuated reflectivities as a function of rainfall rate. As a result, the observed vertical gradients (i.e., vertical derivatives) of measured reflectivity are caused mainly by attenuation, and the slope of the vertical profiles of CloudSat reflectivity profiles can be related to the attenuation coefficient. This slope is estimated using the LSM procedure for the data at several consecutive CloudSat resolution gates (typically three to five gates). The attenuation coefficient is then related to rainfall rate.

The main sources of uncertainty of this method are the variability of the attenuation coefficient–rainfall-rate relation due to DSD changes, the variability in nonattenuated reflectivities at the slope estimation interval, and multiple-scattering effects. The errors due to the first two contributions are random in nature and can amount to about 40%–50% retrieval uncertainties for  $R$  greater than about 2–3 mm h<sup>-1</sup>. Retrieval uncertainties may increase for lower rainfall rates as attenuation in rain becomes weaker, attenuation contributions from cloud liquid water become relatively more important, and variability in nonattenuated W-band reflectivity increases due to diminishing non-Rayleigh scattering effects. Application of the suggested method to rains with  $R \sim 1$ –2 mm h<sup>-1</sup>, however, indicated that sensible CloudSat retrievals can be performed with the attenuation-based method even for such light rainfalls.

Multiple scattering, while not an issue for airborne W-band radars, tends to increase the observed reflectivities due to the rather crude spatial resolution of CloudSat measurements. Although multiple scattering is manifested much stronger in the absolute values of

observed reflectivities, the reflectivity gradients tend to decrease compared to what would be observed if only single scattering were present. As a result, the rainfall-rate retrievals may be biased low if MS effects are not taken into account.

A relatively simple approach to correct attenuation-based retrievals for MS effects has been suggested based on Monte Carlo simulations of CloudSat measurements. The MS bias correction increases with rainfall rate, and it is rather minor (typically within 10% or so for  $R$  less than about 5 mm h<sup>-1</sup>). For a given rainfall rate, this correction increases with the height of the freezing level. It amounts to about 20% for  $R \sim 8$ –10 mm h<sup>-1</sup> (FL  $\sim 4$  km). For heavier rainfalls ( $R \sim 20$ –25 mm h<sup>-1</sup>) and thick rain layers, the MS correction can increase rainfall-rate estimates by a factor of 2 or so compared to retrievals under the SS assumption. This correction also tends to increase in lower parts of rain layers, as MS effects there are stronger than those in the rainfall upper parts. The suggested correction is suited better for stratiform rains resulting from melting snow with a limited degree of riming. Stratiform rain events often exhibit brightband features with the highest reflectivity typically observed near the freezing level, and they usually produce rainfall rates less than about 15 mm h<sup>-1</sup>. Convective rains are likely to have a strong vertical variability, include high-density graupel, and have significant amounts of cloud liquid water. All these factors would affect the magnitude of MS correction and might result in higher uncertainties of the suggested correction.

For rainfalls with  $R > 25$  mm h<sup>-1</sup>, MS effects in CloudSat measurements become so dominant that observed reflectivities (and their vertical derivatives) change little with further increases in precipitation intensity. As a result, rainfall retrievals using the method suggested here (and quite likely any other CloudSat-based method) become very problematic except for shallow rain layers where retrievals can, probably, be extended to somewhat higher values of  $R$ . The combination of high rain intensity and lower freezing-level heights is, however, not a very common occurrence.

The application of the suggested method to a case study covering a relatively wide range of rainfall rates indicated a general robustness of the attenuation-based gradient method. Comparisons of CloudSat retrievals with data from conventional ground-based scanning precipitation radars operating S-band frequencies, which was performed here and in previous studies (Matrosov 2007b) provided a general agreement that was well within retrieval uncertainties. While these comparisons cannot be regarded as a strict complete validation of CloudSat rainfall retrievals, they are a neces-

sary step in a validation procedure, because surface radars are one of only a few tools that are able to provide spatial rainfall estimates. The use of this tool for comparisons with CloudSat is also important because surface radar networks are increasingly used for QPE.

The differential character of measurements of the suggested method makes it immune to such factors as absolute radar calibration and attenuation in snow and melting layer, which can be substantial (e.g., Matrosov 2008). The application of the method does not depend on the type of the surface because it does not require surface returns. More theoretical and experimental studies, however, are needed to fully understand the applicability range and limitations of this method and to refine MS corrections, especially in lower parts of heavier rainfalls with high FL heights and for situations when the cloud liquid water contribution is important. Considering nonuniform beamfilling effects and developing MS corrections for special types of rainfalls such as those when snowflake melting is not a dominant rain formation mechanism (e.g., convective rains) also deserves a separate study. Other outstanding issues include assessing the influence of hydrometer nonsphericity and size distribution variations on MS corrections. Future comparisons with other potential CloudSat methods for rainfall will be a necessary step in evaluating the attenuation-based method.

*Acknowledgments.* This research was funded through NASA Project NNX07AQ82.

#### REFERENCES

- Battaglia, A., and C. Simmer, 2008: How does multiple scattering affect the spaceborne W-band radar measurements at ranges close to and crossing the sea surface range? *IEEE Trans. Geosci. Remote Sens.*, **46**, 1644–1651.
- , M. O. Ajewole, and C. Simmer, 2007: Evaluation of radar multiple scattering effects in CloudSat configuration. *Atmos. Chem. Phys.*, **7**, 1719–1730.
- Bellon, A. G., W. Lee, and I. Zawadzki, 2006: Error statistic of VPR corrections in stratiform precipitations. *J. Appl. Meteor.*, **44**, 988–1015.
- Hitschfeld, W., and J. Bordan, 1954: Errors inherent in the radar measurements of rainfall at attenuating wavelengths. *J. Meteor.*, **11**, 58–67.
- Iguchi, T., T. Kozu, R. Meneghini, J. Awaka, and K. Okamoto, 2000: Rain-profiling algorithm for the TRMM precipitation radar. *J. Appl. Meteor.*, **39**, 2038–2052.
- L'Ecuyer, T. S., and G. L. Stephens, 2002: An estimation-based precipitation retrieval algorithm for attenuating radars. *J. Appl. Meteor.*, **41**, 272–285.
- Li, L., G. M. Heymsfield, P. E. Racette, L. Tian, and E. Zenker, 2004: A 94-GHz cloud radar system on a NASA high-altitude ER-2 aircraft. *J. Atmos. Oceanic Technol.*, **21**, 1378–1388.
- Mace, G. G., R. Marchand, Q. Zhang, and G. Stephens, 2007: Global hydrometeor occurrence as observed by CloudSat: Initial observations from summer 2006. *Geophys. Res. Lett.*, **34**, L09808, doi:10.1029/2006GL029017.
- Matrosov, S. Y., 2007a: Modeling backscatter properties of snowfall at millimeter wavelengths. *J. Atmos. Sci.*, **64**, 1727–1736.
- , 2007b: Potential for attenuation-based estimations of rainfall rate from CloudSat. *Geophys. Res. Lett.*, **34**, L05817, doi:10.1029/2006GL029161.
- , 2008: Assessment of radar signal attenuation caused by the melting hydrometeor layer. *IEEE Trans. Geosci. Remote Sens.*, **46**, 1039–1047.
- , D. E. Kingsmill, B. E. Martner, and F. M. Ralph, 2005: The utility of X-band polarimetric radar for quantitative estimates of rainfall parameters. *J. Hydrometeorol.*, **6**, 248–262.
- , P. T. May, and M. D. Shupe, 2006: Rainfall profiling using Atmospheric Radiation Measurement Program vertically pointing 8-mm wavelength radars. *J. Atmos. Oceanic Technol.*, **23**, 1478–1491.
- , K. A. Clark, and D. E. Kingsmill, 2007: A polarimetric radar approach to identify rain, melting layer, and snow regions for applying corrections to vertical profiles of reflectivity. *J. Appl. Meteor. Climatol.*, **46**, 154–166.
- , M. D. Shupe, and I. V. Djalalova, 2008: Snowfall retrievals using millimeter-wavelength cloud radars. *J. Appl. Meteor. Climatol.*, **47**, 769–777.
- Meneghini, R., T. Iguchi, T. Kozu, L. Liao, K. Okamoto, J. A. Jones, and J. Kwiatkowski, 2000: Use of the surface reference techniques for path attenuation estimates from TRMM precipitation radar. *J. Appl. Meteor.*, **39**, 2053–2070.
- Sassen, K., S. Y. Matrosov, and J. Campbell, 2007: CloudSat space borne 94 GHz radar bright band in the melting layer: An attenuation-driven upside-down lidar analog. *Geophys. Res. Lett.*, **34**, L16818, doi:10.1029/2007GL030291.
- Stephens, G. L., and Coauthors, 2002: The CloudSat mission and the A-train. A new dimension of space observations of clouds and precipitation. *Bull. Amer. Meteor. Soc.*, **83**, 1771–1790.
- Testud, J., E. Le Bouar, E. Obligis, and M. Ali-Mehenni, 2000: The rain profiling algorithm applied to polarimetric weather radar. *J. Atmos. Oceanic Technol.*, **17**, 332–356.